

Published in final edited form as:

Nat Commun. ; 6: 6243. doi:10.1038/ncomms7243.

A cnidarian homologue of an insect gustatory receptor functions in developmental body patterning

Michael Saina¹, Henriette Busengdal², Chiara Sinigaglia^{2,4}, Libero Petrone³, Paola Oliveri^{3,*}, Fabian Rentzsch^{2,*}, and Richard Benton^{1,*}

¹Center for Integrative Genomics Faculty of Biology and Medicine University of Lausanne CH-1015 Lausanne Switzerland ²Sars Centre for Marine Molecular Biology University of Bergen Bergen N-5008 Norway ³Departments of Genetics, Evolution & Environment and Cell and Developmental Biology University College London London WC1E 6BT United Kingdom

Abstract

Insect Gustatory and Odorant Receptors (GRs and ORs) form a superfamily of novel transmembrane proteins, which are expressed in chemosensory neurons that detect environmental stimuli. Here we identify homologues of *GRs* (*Gustatory receptor-like (Grl)* genes) in genomes across Protostomia, Deuterostomia and non-Bilateria. Surprisingly, two *Grls* in the cnidarian *Nematostella vectensis*, *NvecGrl1* and *NvecGrl2*, are expressed early in development, in the blastula and gastrula, but not at later stages when a putative chemosensory organ forms. *NvecGrl1* transcripts are detected around the arboral pole, considered the equivalent to the head-forming region of Bilateria. Morpholino-mediated knockdown of *NvecGrl1* causes developmental patterning defects of this region, leading to animals lacking the apical sensory organ. A deuterostome *Grl* from the sea urchin *Strongylocentrotus purpuratus* displays similar patterns of developmental expression. These results reveal an early evolutionary origin of the insect chemosensory receptor family, and raise the possibility that their ancestral role was in embryonic development.

Introduction

The insect chemosensory receptor superfamily, including Gustatory Receptors (GRs) and Odorant Receptors (ORs) (which represent an expanded clade within the GR family¹), are polytopic membrane proteins responsible for detecting a vast number of non-volatile and

Users may view, print, copy, and download text and data-mine the content in such documents, for the purposes of academic research, subject always to the full Conditions of use:http://www.nature.com/authors/editorial_policies/license.html#terms

*Corresponding authors: Richard.Benton@unil.ch Fabian.Rentzsch@sars.uib.no P.Oliveri@ucl.ac.uk.

⁴Present address: Developmental Biology Unit Observatoire Océanologique 06234 Villefranche-sur-mer France

Author contributions M.S. conceived the project, performed bioinformatics analyses, and qPCR, morpholino injections and *in situ* hybridisations in *N. vectensis*, analysed data and wrote the manuscript. H.B. performed gene cloning, morpholino injections and *in situ* hybridisations in *N. vectensis*. C.S. performed morpholino injections and *in situ* hybridisations in *N. vectensis*. L.P. performed qPCR and *in situ* hybridisations in *S. purpuratus*. P.O. designed and performed qPCR and *in situ* hybridisations in *S. purpuratus*, analysed data and contributed to writing the manuscript. F.R. performed morpholino injections and *in situ* hybridisations in *N. vectensis*, analysed data and contributed to writing the manuscript. R.B. conceived and supervised the project, analysed data and wrote the manuscript.

Competing financial interests: The authors declare no competing financial interests.

volatile chemicals in the environment^{2, 3}. Most sequenced insect genomes are predicted to encode several dozen to a few hundred highly divergent GRs and/or ORs⁴. Almost all of these receptors are likely to be expressed in small subsets of sensory neurons in peripheral chemosensory organs. Here they recognise external chemical cues – including esters, alcohols, ketones and volatile lipid-derived pheromones (for ORs), and sugars, bitter compounds and cuticular pheromones (for GRs) – to permit perception of food, environmental dangers, kin and potential mates^{5, 6}. A few exceptional GRs have either internal chemosensing or other sensory functions⁷⁻⁹. In the presence of their cognate ligands, these receptors induce neuronal firing, although their signalling mechanism is poorly understood. ORs are thought to function as odour-gated ion channels^{10, 11}, formed by a complex of an odour-specific OR and a co-receptor, ORCO¹². GRs are less well-characterised molecularly: while they are also likely to function ionotropically¹³, it remains unclear if they function alone or in complexes of co-expressed GR subunits¹⁴.

Understanding the molecular mechanism by which GRs and ORs act has been hampered by their lack of sequence similarity to either known ion channels or other types of membrane protein. The receptors are predicted to contain seven transmembrane domains, similar to G protein-coupled receptors (GPCRs). Their membrane topology is, however, inverted compared to GPCRs, defining them as a distinct class of transmembrane protein^{12, 15, 16}. Thus, despite the widespread function for insect chemosensory receptors in mediating perception of the external chemical world, the genesis of this protein family is unknown.

In this work, we have used comparative genomics to characterise the evolutionary origins and dynamics of this family of receptors, and experimental analyses of GR homologues in species distant from insects to reveal an unexpected role for these proteins during embryonic development.

Results

Deep conservation of gustatory receptor-like (*Grl*) genes

We performed TBLASTN and PSI-BLAST searches using insect GRs and ORs as queries to identify putative homologous genes within non-insect genomes available at NCBI and other public genome and Expressed Sequence Tag (EST) databases (see Methods) (Figure 1a, Supplementary Table 1 and Supplementary Data 1). Within Protostomia, these searches recovered the previously described GRs of the crustacean *Daphnia pulex* (water flea)¹⁷ and the *gustatory related (gur)* and *serpentine receptor class R (srr)* genes of *C. elegans*^{1, 18, 19} and other nematodes. Beyond Ecdysozoa, we identified what we term GR-like (*Grl*) genes in Lophotrochozoa, including the annelids *Capitella teleta* (polychaete worm) and *Helobdella robusta* (freshwater leech)²⁰, and the molluscs, *Lottia gigantea* (owl limpet)²⁰, *Crassostrea gigas* (Pacific oyster)²¹ and *Aplysia californica* (sea slug). We also found homologous genes in Deuterostomia, including the hemichordate *Saccoglossus kowalevskii* (acorn worm) and several echinoderms, including the sea urchin *Strongylocentrotus purpuratus*²², but not in any chordate (Fig. 1a). Finally, we identified a small number of *Grl* genes in non-bilaterian species, including Cnidaria, such as the sea anemone *Nematostella vectensis*²³ (independently noted in another study²⁴) and the corals *Acropora digitifera*²⁵ and *Acropora millepora*, and the placozoan *Trichoplax adhaerens*²⁶. No sequences were

recovered, however, from the genomes of another cnidarian, *Hydra magnipapillata*, the ctenophores *Mnemiopsis leidyi*²⁷ and *Pleurobrachia bachei*²⁸, or the sponges *Amphimedon queenslandica*²⁹ and *Oscarella carmela*³⁰. No fungal, unicellular eukaryotic or prokaryotic genomes contained identifiable Grls (Fig. 1a).

Several observations support the classification of the identified genes as *Grls*. First, reciprocal BLAST with each Grl sequence against insect genomes identified an insect GR as the most significant hit. Second, the encoded proteins each contain multiple predicted transmembrane domains (TMDs) – most commonly 6-7 TMDs in putative full-length Grl sequences – similar to GRs and ORs (Fig. 1b). (Accurate computational predictions of TMD number and topology are difficult because of the variable hydrophobicity of TMDs within this family of receptors¹²). Third, the phase and position of three inferred ancestral introns in the 3' region of *D. melanogaster* GR transcripts¹ are well-conserved in Grls (Fig. 1c). Finally, Grls share a number of characteristic amino acid residues with the most highly conserved C-terminal region of the insect receptors, including a tyrosine residue important for ion channel function in insect ORs³¹ (Fig. 1c).

The overall sequence similarity of Grls and insect GRs (or ORs) is very low (~15-20% amino acid identity, similar to the minimum identity within the GR and OR families themselves¹), with the highest similarity to the GR64a-f/GR61a clade of sugar-sensing receptors¹⁴. Phylogenetic analysis revealed no unambiguous orthologous relationships of Grls with any insect GR, or between Grls of different lophotrochozoan, deuterostome or non-bilaterian species (Fig. 2). Although the high divergence of these sequences precludes accurate reconstruction of their ancestry, many members of these repertoires appear to have formed by species-specific expansions (Fig. 2).

Early developmental expression of *Grl* genes in *N. vectensis*

To investigate the role of Grls in non-Arthropoda, we focused in this study on the cnidarian *N. vectensis* (here abbreviated *Nvec*), which is amenable to gene expression and functional analyses. Moreover, the development and anatomy of this organism are relatively well-described, and a presumed chemosensory structure, the apical organ, has been identified (Fig. 3a)^{32, 33}. *N. vectensis* development proceeds through a coeloblastula stage to gastrulation, which occurs mainly by invagination^{34, 35}. After gastrulation, the embryo emerges from the egg jelly as a free-swimming planula, which moves by ciliary beating with the apical sense organ pointing forward. Subsequently, the planula transforms (“metamorphoses”) into a sessile polyp, which starts feeding after formation of the tentacles that surround the single opening of the animal (Fig. 3a).

Surprisingly, analysis of the temporal pattern of expression of the two *Grls* we found in this species, *NvecGrl1* and *NvecGrl2*, by quantitative RT-PCR (qPCR) revealed the highest level of expression of these genes in early developmental stages (Fig. 3b and Supplementary Table 2): *NvecGrl1* is expressed in the egg and blastula, gastrula and early planula stages, diminishing rapidly to undetectable levels later in development. *NvecGrl2* is only robustly detected in the egg and blastula. These temporal expression profiles contrast markedly with those of *D. melanogaster* GRs and ORs, where expression of these receptors has been reported only in differentiated sensory neurons⁵.

We next examined the spatial distribution of *N. vectensis* *Grl* transcripts by whole mount RNA *in situ* hybridisation on a range of developmental stages. While *NvecGrl2* RNA was undetectable in these experiments (Supplementary Fig. 1), we first observed *NvecGrl1* transcripts in a broad aboral domain³⁶ at gastrula stage (Fig. 3c). This domain develops under the control of genes homologous to those that regulate anterior (or apical) development in bilaterians³⁶, and its centre is the site of formation of the apical sensory organ in the planula larva (Fig. 3a). Genes with similarly broad aboral expression at the gastrula stage display different expression dynamics after gastrulation: “spot genes” (for example, *NvecFgfa1*, *NvecFgfa2* and *NvecSoxB1*) become restricted to a small spot at the aboral pole, from which the apical organ develops, whereas “ring genes” (for example, *NvecSix3/6* and *NvecFoxQ2a*) remain expressed in a ring-like domain around the apical organ³⁶. Comparison of the spatial distribution of *NvecGrl1* with *NvecFGFa1* by double RNA *in situ* hybridisation revealed that the *NvecGrl1* expression domain remains broad at late gastrula/early planula stages when *NvecFgfa1* has already restricted to a small aboral spot (Fig. 3d). Subsequently, *NvecGrl1* transcripts are excluded from the apical organ-forming spot (Fig. 3e), similar to other “ring genes”. While the “ring gene” domain includes some scattered sensory cells^{37, 38}, the broad and early expression of *NvecGrls* in the aboral domain indicates that these receptors may primarily have nonchemosensory roles in this species.

Regulation of *NvecGrl1* by the aboral patterning network

Several transcription factors and signalling molecules that are expressed in the aboral region and required for apical organ formation in *N. vectensis* have been identified³⁶. For example, the homeodomain transcription factor *NvecSix3/6* is an important determinant of the aboral territory, where it initiates an autoregulatory loop of Fibroblast Growth Factor (FGF) signalling to pattern this domain³⁶. To determine if *NvecGrl1* aboral expression is regulated by these factors, we performed RNA *in situ* hybridisation on zygotes injected with morpholino oligonucleotides (morphants) designed to block translation of these genes. In *NvecSix3/6* morphants, *NvecGrl1* aboral expression is reduced or absent in gastrula embryos compared to control morphants, similar to other markers of this domain³⁶ (Fig. 4a), suggesting that *NvecGrl1* functions downstream of this transcription factor.

NvecFgfa1 and *NvecFgfa2* participate in positive and negative feedback regulation of apical organ formation, respectively^{33, 36}: *NvecFgfa1* morphants fail to develop an apical organ³³, whereas *NvecFgfa2* morphants display precocious formation of an expanded apical organ³⁶. However, while effects of *NvecFgfa1* knockdown become visible only after gastrulation, an expansion and/or up-regulation of apical organ domain genes in *NvecFgfa2* knockdown animals is detectable already at gastrula stage³⁶. Consistently, we found that the expression of *NvecGrl1* appears only slightly affected in *NvecFgfa1* morphants at the end of gastrulation (Fig. 4b). By contrast, in *NvecFgfa2* morphants, *NvecGrl1* expression forms an expanded ring with a wider area of low *NvecGrl1* expression in its centre and this ring-like domain appears earlier than in control animals (Fig. 4c; compare with Fig. 3e). These data provide further evidence that *NvecGrl1* is expressed in cells that do not directly give rise to the apical sensory organ.

Grl1* is required for aboral patterning in *N. vectensis

To investigate the function of *NvecGrl1*, we injected zygotes with morpholino oligonucleotides designed to block translation of this receptor, and examined development of these animals in parallel with those injected with control morpholinos (see Methods). Early developmental processes, including gastrulation, appeared to proceed normally in both *NvecGrl1* and control morphant animals (Fig. 5a). However, *NvecGrl1* morphants displayed pronounced morphological defects in the apical organ domain in planula larvae (Fig. 5a-b). In control animals, the first sign of apical organ formation is the translocation of the nuclei in a small group of cells at the aboral pole to a more basal position (Fig. 5a). These cells subsequently form a small indentation of the aboral ectoderm (Fig. 5a); this indentation is the site from which the long cilia of the apical organ emerge³⁷. In *NvecGrl1* morphants the initial basal movement of nuclei is absent or strongly reduced and no clear indentation develops (Fig. 5a). Correspondingly, the apical tuft is absent or consists of only few long cilia in 4 day-old *NvecGrl1* morphants (Fig. 5b). These animals subsequently fail to develop into primary polyps (0%, n = 159 *NvecGrl1* morphants, compared to control morphants 63%, n = 122). These defects were reproduced with a second morpholino against *NvecGrl1* (<9% primary polyps, n = 109).

To understand the basis for these morphological defects, we analysed expression of aboral domain patterning genes in *NvecGrl1* morphants. *NvecSix3/6* expression is greatly diminished – but not abolished – in *NvecGrl1* morphants at the planula stage compared to control morphants (Fig. 5c). Consistent with the reduction of *NvecSix3/6* expression, two of its downstream targets, the transcription factor *NvecFoxQ2a* and *NvecFgfa2*³⁶, are also reduced in *NvecGrl1* morphants compared to controls (Fig. 5c). Defects in gene expression were also detectable at gastrula stages (Supplementary Fig. 2a), when *NvecGrl1* transcripts are first detected in the aboral domain, although these phenotypes were very subtle, though consistent, for *NvecSix3/6* and *NvecFoxQ2a*. Together, these observations implicate *NvecGrl1* in a feedback pathway that maintains *NvecSix3/6* expression to pattern the aboral domain. By contrast, patterning genes expressed elsewhere in the embryo, for example, *NvecWnt2*, which is found in a belt-like domain between the aboral and oral poles³⁹, are not or at most mildly affected in *NvecGrl1* morphants (Fig. 5c).

One of the important functions of the FGF signalling loop is to down-regulate *NvecSix3/6* expression after gastrulation in a small “spot”, the developing apical organ domain. Within this spot, genes required for apical organ formation, such as the transcription factor *NvecHoxF*, are expressed³⁶. Defects in the initiation of FGF signalling leads to a failure in formation of this *NvecSix3/6*- and *NvecFoxQ2*-negative and *NvecHoxF*-positive aboral spot³⁶. We observed a similar phenotype in *NvecGrl1*, but not control, morphants (Fig. 5c and Supplementary Fig. 2b); these defects could account for failure of apical organ development. Together, these results support a role for *NvecGrl1* in the regulatory network that controls aboral domain patterning and thereby apical sensory organ formation.

Developmental expression of a deuterostome *Grl* gene

To determine whether the early developmental expression of *Grl* genes is conserved in Deuterostomia, we used qPCR to analyse transcript levels of the five *Grls* of the echinoderm

S. purpuratus during embryonic stages (Fig. 6a). Notably, *SpurGrll*, which is the most similar sea urchin *Grl* to *NvecGrll* (Fig. 2), was detected during early development (Fig. 6b and Supplementary Table 3): the highest expression of *SpurGrll* was at the blastula stage, but it remained at elevated levels in the gastrula and later embryonic developmental stages. These qPCR data are in agreement with quantitative developmental transcriptome data (Supplementary Fig. 3a)⁴⁰. The other four *SpurGrls* were expressed at only very low levels during developmental stages (Fig. 6b), but transcripts could be readily amplified for all *SpurGrls*, except *SpurGrl3*, from adult neural tissue (Supplementary Fig. 3b). These observations suggest that *SpurGrll* has a unique function during embryonic development.

By whole mount RNA *in situ* hybridisation, we observed that *SpurGrll* exhibits a dynamic, spatial expression pattern during early development (Fig. 6c). In the blastula, *SpurGrll* RNA was present ubiquitously, while in later stages, it was restricted to few groups of cells. From the late gastrula, transcripts were detected in cells in the apical domain, which develops into a neurosensory structure⁴¹. Strong *SpurGrll* expression was also detected in two bilaterally arrayed cells in the oral ectoderm and, at lower levels, in the hindgut and adjacent ectoderm, as well as a region of the aboral ectoderm that will develop into the vertex (Fig. 6c). The apical domain expression of *SpurGrll* represents an intriguing parallel with that of *NvecGrll* in the developmentally-equivalent region of the sea anemone gastrula^{36, 42, 43}, although the additional expression patterns suggest that the sea urchin gene has several functions.

Discussion

We have defined an early evolutionary origin and broad phylogenetic distribution of the insect chemosensory receptor superfamily. Previously only characterised in Ecdyosozoa^{2, 17, 44, 45}, we show *GR-like (Grl)* genes are present in genomes across Protostomia, non-chordate Deuterostomia and non-Bilateria. These observations establish the origin of this gene family prior to the split of Bilateria and non-Bilateria 550-850 million years ago⁴⁶, and suggest that these genes have been lost in the ancestral chordate.

Through analysis of *Grls* in the non-bilaterian *N. vectensis*, we found – unexpectedly – several lines of evidence supporting a role in developmental body patterning rather than external chemosensation. First, the existence of a small number of *NvecGrls* is inconsistent with this cnidarian receptor repertoire playing a wide-ranging role in the detection of environmental chemical signals, like their insect homologues. We note that *N. vectensis* has several dozen vertebrate OR-like GPCRs, which represent candidate chemosensory receptors of this species⁴⁷. Second, in contrast to *Drosophila* ORs and GRs⁴⁸, both *NvecGrls* are expressed in early developmental stages, prior to formation of sensory neurons and a putative chemosensory organ (at late gastrula and mid-planula stage, respectively^{37, 38}). Moreover, *NvecGrll* transcripts are detected broadly around the aboral pole in gastrula and planula stages, but are selectively excluded from an aboral “spot” of cells that subsequently gives rise to the apical sensory organ. Third, functional analysis of *NvecGrll* supports a role in aboral body patterning essential for developmental progression. While our data argue that *NvecGrls* have a different function to insect GRs, we cannot

exclude that they have a later, additional role, for example in the detection of metamorphosis-related sensory signals.

Although loss of *NvecGr11* blocks developmental progression beyond the planula stage, the relatively limited current knowledge of aboral patterning in Cnidaria makes it difficult to define the precise role of this protein. Our data are consistent with a model in which *NvecGr11* functions downstream of the aboral territory determinant *NvecSix3/6* in the feedback loop that is important to refine aboral pole patterning and promote apical organ formation³⁶. Secondary structure and sequence conservation of *NvecGr11* (and other Gr1s) with insect GRs and ORs suggest that this protein acts as a ligand-gated ion channel, and might recognise a paracrine developmental signal; testing this model will require identification of a relevant ligand. Nevertheless, it is intriguing that *NvecGr11* plays a role in the formation (albeit indirectly) rather than the function, of a putative chemosensory organ. We have not been able to detect transcripts for *NvecGr12* gene *in situ* and morpholino-mediated knock-down of *NvecGr12* did not reveal any obvious patterning defects (unpublished data), suggesting that this gene has a different role to *NvecGr11*.

The similarities in the early developmental expression of the deuterostome Gr1 gene with highest sequence identity to *NvecGr11*, *S. purpuratus Gr11*, hints that a role in embryonic patterning may have been an ancestral function of this family. However, *SpurGr11* displays additional spatial expression patterns beyond the apical domain, and four additional *SpurGr1s* do not show such early expression, suggesting that Gr1s in this species have multiple different roles. Cleanly dissecting the function of *SpurGr11* (and its paralogues) will require methods that permit tissue-specific gene knockdown.

Beyond the work presented here, very little is known about the role of members of the GR/Gr1 family outside insects. The large size and high sequence divergence of the GR repertoire in the crustacean *D. pulex* is consistent with a role in chemosensation¹⁷, although no expression or functional analyses of these receptors have been reported. The nematode *C. elegans* relies on a very large family of GPCRs for chemical detection¹⁸, and of the fifteen GR-like genes (the *gur* and *srr* families^{1, 18, 19}, the latter not previously defined as members of this superfamily), only two have been characterised. GUR-2 (also known as LITE-1) functions in photosensitive neurons^{44, 45}, although it has not been determined whether this protein senses light directly. GUR-1 (also known as EGL-47) appears to regulate motoneurons that control egg-laying⁴⁹. Together with our data in *N. vectensis* and *S. purpuratus*, these observations suggest that Gr1/GR-genes may have been recruited only in arthropods to fulfil a predominant role in peripheral chemosensation. Future analysis of other Gr1s in a range of species should yield insights into the diverse functions and evolutionary history of this unusual receptor family.

Methods

Gene identification

To identify homologues of insect chemoreceptors, all known *Drosophila* sequences of GRs and ORs were used as queries in extensive TBLASTN and PSI-BLAST searches of public genome and EST datasets (see Supplementary Table 1 and Supplementary Data 1) and in

screens of OrthoDB⁵⁰. Identified genes were used in iterative BLAST searches of species-specific datasets until no new sequences were identified. The number of genes in most species are likely to represent minimum estimates due to the challenge of identifying highly divergent *Grl* genes from incompletely assembled genomes with computational predictions alone. For the same reasons, most predicted sequences are incomplete, particularly at the more divergent 5' end. Analysis of the membrane topology (excluding partial protein sequences) was performed using TMHMM v.2.0⁵¹. Intron positions and phases were predicted by comparing cloned (or predicted) transcript sequences and the corresponding genomic sequences.

Alignment/phylogenetic tree building

Protein alignments were built using Clustal Omega⁵² with the following settings: max HMM Iterations: 5; combined iterations: 5; max guide iterations: 5. The N-termini of the sequences were cut off after aligning using Jalview⁵³ and only the C-terminal regions from transmembrane domain 5 (starting with position 352 in DmelORCO) was used for further analysis. Tree reconstruction was performed using PhyML3.0⁵⁴ and the LG model⁵⁵ was used as a substitution matrix. Branch support was calculated using the Approximate Likelihood-Ratio Test method⁵⁶. The tree was rooted on the Rhodopsin branch, although we acknowledge that the evolutionary relationship between these receptor families is still unclear.

Cloning of full-length *Grl* coding sequences

To obtain the complete coding sequence of *NvecGrl1*, PCR was performed on mixed embryo stage cDNA with specific primers based on EST and genome data (genome.jgipsf.org/Nemve1/Nemve1.home.html). For *NvecGrl2* 5' and 3' RACE PCRs were performed. The following primer sets were used:

NvecGrl1

5': GTGTGAGCACGCTGCGAGAATGG

3': TCACTTAAACTGGACAAGAATCG

NvecGrl2

5'RACE outer primer: AGAGCAGAAGGCTCACAAGC

5'RACE inner primer: CAAGGAATTCATTGCGACAG

3'RACE outer primer: CGATTGGAGGAATTGTCCCAGTAACACGCGG

3'RACE inner primer: TCAACACAGAAGTGATCAGCCCAACGATTGG

Genbank accession numbers are: KP294348 (*NvecGrl1*) and KP294349 (*NvecGrl2*).

For *SpurGr11*, a 1212 bp fragment of the coding sequence was amplified by PCR from 18 hpf embryonic cDNA, cloned into pGEM-T Easy (Promega) and sequenced, using the following primers designed on the WHL22.291934 transcriptome sequence:

5': GAACACCACTCCATGGAACC

3': CTATGGGATCACCGCTCACT

Quantitative PCR

For *N. vectensis*, cell lysates of embryonic stages were collected and the total RNA was extracted using the RNAqueous kit (Ambion). cDNA synthesis was performed using the SuperScript II RT Reagent Kit according to the manufacturer's protocol. Expression of *NvecGr11*, *NvecGr12* and reference genes were analysed by performing PCR on an Applied Biosystems 7900HT SDS using the cDNA as template and SYBR Premix (Roche) with the following primers:

NvecGr11

5': AATCGTGCTAGCCACATTCTGGTG

3': ACCTCGTACACAACGCCTGTCAAA

NvecGr12

5': ACTATAGTAACGTCACCTTGCGGGTGC

3': TTCGCCGTCTTTTCAGTTCATCCAC

Ef1b

5': TGCTGCATCAGAACAGAAACCTGC

3': TAAGCCTTCAAGCGTTCTTGCCTG

RibPrL23

5': TTACGGAGCTCTGGCTTTCCTTTC

3': TGCCGTTAAGGGTATCAAAGGACG

The reference target stability values were as follows EF1alpha (M = 0.404; CV = 0.135), RibPr23L (M = 0.404; C = 0.144), average (M = 0.404; CV = 0.140).

For *S. purpuratus*, cell lysates of appropriately-staged embryos were collected and total RNA was extracted using the RNeasy Micro Kit (Qiagen). cDNA synthesis was performed using the iScript™ cDNA Synthesis Kit (Bio-Rad) according to the manufacturer's instructions. At least four technical replicas were run on two independent cDNA batches, using cDNA equivalent to 1 embryo per reaction (2.8 ng) and Power SYBR® Green QPCR

master mix (Applied Biosystems), on the 7900HT Fast Real-Time PCR system and the following primers (*SpurUbq* was used as internal standard^{57, 58}):

SpurGr1

5': TCTGCGAATCGAGAAGTCCT

3': GAGCCATAGTCGCGTAGGTC

SpurGr2

5': CATCCACGGTCTGAAGACAA

3': GCAACTTGAAACGCCCATAC

SpurGr3

5': GCCTCAATTTAGCGGCAGTA

3': CCAGATAGGATGTGGCAGGT

SpurGr4

5': ATCCTCAGCCCTTTCTGACA

3': GAACTGGTCGGTCAGGATGT

SpurGr5

5': ATAACGCTGAGCCGGTACAA

3': TGGTTGCAGCAGTTTGAAAG

SpurUbq

5': CACAGGCAAGACCATCACAC

3': GAGAGAGTGCGACCATCCTC

Morpholinos

Translation-blocking antisense morpholino oligonucleotides (GeneTools, LLC) were designed to match the sequence of *NvecGr11*. The sequences of the morpholinos used are:

NvecGr11#1: ACGCTCCGACTGGAACTGCCATTCA

NvecGr11#2: GAACTGCCATTCATTCCGCTTGTTTC

control#1 (generic;³⁶): CCATTGTGAAGTTAAACGATAGATC

control#2 (*NvecGr11* mismatch): ACGCGCCTACTGGAATTGCTATTAA

The two morpholinos against *NvecGr11* are partially overlapping to avoid 5'UTR sequence that is present elsewhere in the genome. The sequence corresponding to the start codon in the *NvecGr11* morpholinos is underlined.

Six3/6: GTACTGCCGCACTGCAAGACTTGTC³⁶

Fgfa1: ATAAGGTGGACGCATGACTTTGTAG

Fgfa2: CGTTAGCATGGTGATCGTCATGTTG³³

***Nematostella* culture, manipulation and microinjection**

Animals were cultured at 18°C in 1:3 diluted sea water in the Sars Centre Cnidaria facility, and gamete production was induced by overnight exposure to light and elevated temperature (25°C)⁵⁹. Morpholinos were diluted in H₂O, together with a tracer (Alexa568 Dextran (Molecular Probes) at 0.1 mg/ml), to a final concentration of either 1 mM (*NvecGr11*#1) or 0.6 mM (*NvecGr11*#2); control morpholinos were diluted to the same concentration in parallel experiments. Zygotes were microinjected using an Eppendorf Femtojet, with a volume equivalent to approximately 5% of the egg. Following injections, the embryos were transferred to Petri dishes containing *Nematostella*-medium and allowed to develop at 21°C until fixation. For images of live planulae, animals were mounted in 2% methylcellulose (in *Nematostella* Medium) and imaged on a Nikon Eclipse E800 microscope.

Histology

N. vectensis: for actin and DNA staining, specimens were fixed in 4% formaldehyde in PBT (0.1% Triton X-100 in PBS) for 1 h and washed four times in PBT. 30 µl of Alexa Fluor 488 Phalloidin (Molecular Probes) were put in an open Eppendorf tube for 30 min at room temperature to let the solvent evaporate. The pellet was redissolved in 1.5 ml PBT and 1.5 µl TO-PRO-3 Iodide (Molecular Probes) was added. The specimens were incubated for 2-3 h in this staining solution, washed five times with PBT, and mounted in ProLong Gold (Life Technologies). RNA *in situ* hybridisation on *N. vectensis* was performed using antisense digoxigenin-labelled probes against the open reading frame (ORF) of the desired genes essentially as described⁶⁰. In brief, hybridisation was carried out at 60°C for 60 hours, and post-hybridisation stringency washes were with 0.01×SSCT. Anti-digoxigenin Fab fragments (Roche) were diluted 1:5000 prior to detection by NBT/BCIP staining (Roche). For *N. vectensis* double *in situ* hybridisation, digoxigenin-labelled *NvecGr11* and FITC-labelled *NvecFGFa1* probes complementary to the corresponding ORF were used. *NvecFGFa1* was detected by NBT/BCIP staining, and *NvecGr11* was detected using anti-DIG-POD and tyramide based signal amplification (TSA[®] plus DNP (AP) kit, Perkin Elmer) followed by anti-DNP-AP-mediated BCIP staining.

S. purpuratus: specimens were fixed in 4% formaldehyde in MOPS buffer overnight at 4°C, then washed several times in MOPS buffer and once in 70% ethanol. After rehydration in TBST, RNA *in situ* hybridisation was performed using an antisense digoxigenin-labelled probe against the 1212 bp fragment of the *SpurGr11* ORF (see above) as described⁶¹. In brief, 0.05 ng/µl of probe was hybridised at 60°C for 16 hours. Post-hybridisation stringency

washes were with $0.1\times\text{SSC}$ and $0.01\times\text{SSC}$. Anti-digoxygenin Fab fragments were diluted 1:2000 prior to detection by NBT/BCIP staining.

Supplementary Material

Refer to Web version on PubMed Central for supplementary material.

Acknowledgements

We are very grateful to Harriet Stephenson for help with the sea urchin RNA *in situ* hybridisation. We acknowledge the Baylor College of Medicine Human Genome Sequencing Center, The Genome Institute at Washington University and the Broad Institute Genome Sequencing Platform for providing prepublication access to genome assemblies. We thank Sophie Martin, Hugh Robertson, Marcus Stensmyr, and members of the Benton lab for discussions and comments on the manuscript. P.O.'s laboratory is supported by University College London and a Human Frontier Science Program Young Investigator Grant. F.R.'s laboratory is supported by the Sars Centre. Research in R.B.'s laboratory is supported by the University of Lausanne, European Research Council Starting Independent Researcher and Consolidator Grants (205202 and 615094) and the Swiss National Science Foundation (31003A_140869).

References

1. Robertson HM, Warr CG, Carlson JR. Molecular evolution of the insect chemoreceptor gene superfamily in *Drosophila melanogaster*. Proc. Natl. Acad. Sci. USA. 2003; 100(Suppl 2):14537–14542. [PubMed: 14608037]
2. Hallem EA, Dahanukar A, Carlson JR. Insect odor and taste receptors. Annu. Rev. Entomol. 2006; 51:113–135. [PubMed: 16332206]
3. Benton R. Chemical sensing in *Drosophila*. Curr. Opin. Neurobiol. 2008; 18:357–363. [PubMed: 18801431]
4. Nei M, Niimura Y, Nozawa M. The evolution of animal chemosensory receptor gene repertoires: roles of chance and necessity. Nat. Rev. Genet. 2008; 9:951–963. [PubMed: 19002141]
5. Vosshall LB, Stocker RF. Molecular Architecture of Smell and Taste in *Drosophila*. Annu. Rev. Neurosci. 2007; 30:505–533. [PubMed: 17506643]
6. Su CY, Menzies K, Carlson JR. Olfactory perception: receptors, cells, and circuits. Cell. 2009; 139:45–59. [PubMed: 19804753]
7. Miyamoto T, Slone J, Song X, Amrein H. A fructose receptor functions as a nutrient sensor in the *Drosophila* brain. Cell. 2012; 151:1113–1125. [PubMed: 23178127]
8. Xiang Y, Yuan Q, Vogt N, Looger LL, Jan LY, Jan YN. Light-avoidance-mediating photoreceptors tile the *Drosophila* larval body wall. Nature. 2010; 468:921–926. [PubMed: 21068723]
9. Ni L, et al. A gustatory receptor paralogue controls rapid warmth avoidance in *Drosophila*. Nature. 2013; 500:580–584. [PubMed: 23925112]
10. Sato K, Pellegrino M, Nakagawa T, Nakagawa T, Vosshall LB, Touhara K. Insect olfactory receptors are heteromeric ligand-gated ion channels. Nature. 2008; 452:1002–1006. [PubMed: 18408712]
11. Wicher D, et al. *Drosophila* odorant receptors are both ligand-gated and cyclic-nucleotide-activated cation channels. Nature. 2008; 452:1007–1011. [PubMed: 18408711]
12. Benton R, Sachse S, Michnick SW, Vosshall LB. Atypical membrane topology and heteromeric function of *Drosophila* odorant receptors *in vivo*. PLOS Biol. 2006; 4:e20. [PubMed: 16402857]
13. Sato K, Tanaka K, Touhara K. Sugar-regulated cation channel formed by an insect gustatory receptor. Proc. Natl. Acad. Sci. USA. 2011; 108:11680–11685. [PubMed: 21709218]
14. Montell C. A taste of the *Drosophila* gustatory receptors. Curr. Opin. Neurobiol. 2009; 19:345–353. [PubMed: 19660932]
15. Zhang HJ, Anderson AR, Trowell SC, Luo AR, Xiang ZH, Xia QY. Topological and functional characterization of an insect gustatory receptor. PLOS ONE. 2011; 6:e24111. [PubMed: 21912618]

16. Lundin C, et al. Membrane topology of the *Drosophila* OR83b odorant receptor. *FEBS Lett.* 2007; 581:5601–5604. [PubMed: 18005664]
17. Penalva-Arana DC, Lynch M, Robertson HM. The chemoreceptor genes of the waterflea *Daphnia pulex*: many Grs but no Ors. *BMC Evol. Biol.* 2009; 9:79. [PubMed: 19383158]
18. Thomas JH, Robertson HM. The *Caenorhabditis* chemoreceptor gene families. *BMC Biol.* 2008; 6:42. [PubMed: 18837995]
19. Robertson HM, Thomas JH. The putative chemoreceptor families of *C. elegans*. *WormBook.* 2006:1–12. [PubMed: 18050473]
20. Simakov O, et al. Insights into bilaterian evolution from three spiralian genomes. *Nature.* 2013; 493:526–531. [PubMed: 23254933]
21. Zhang G, et al. The oyster genome reveals stress adaptation and complexity of shell formation. *Nature.* 2012; 490:49–54. [PubMed: 22992520]
22. Sodergren E, et al. The genome of the sea urchin *Strongylocentrotus purpuratus*. *Science.* 2006; 314:941–952. [PubMed: 17095691]
23. Putnam NH, et al. Sea anemone genome reveals ancestral eumetazoan gene repertoire and genomic organization. *Science.* 2007; 317:86–94. [PubMed: 17615350]
24. Nordstrom KJ, Sallman Almen M, Edstam MM, Fredriksson R, Schioth HB. Independent HHsearch, Needleman--Wunsch-based, and motif analyses reveal the overall hierarchy for most of the G protein-coupled receptor families. *Mol. Biol. Evol.* 2011; 28:2471–2480. [PubMed: 21402729]
25. Shinzato C, et al. Using the *Acropora digitifera* genome to understand coral responses to environmental change. *Nature.* 2011; 476:320–323. [PubMed: 21785439]
26. Srivastava M, et al. The *Trichoplax* genome and the nature of placozoans. *Nature.* 2008; 454:955–960. [PubMed: 18719581]
27. Ryan JF, et al. The genome of the ctenophore *Mnemiopsis leidyi* and its implications for cell type evolution. *Science.* 2013; 342:1242592. [PubMed: 24337300]
28. Moroz LL, et al. The ctenophore genome and the evolutionary origins of neural systems. *Nature.* 2014; 510:109–114. [PubMed: 24847885]
29. Srivastava M, et al. The *Amphimedon queenslandica* genome and the evolution of animal complexity. *Nature.* 2010; 466:720–726. [PubMed: 20686567]
30. Nichols SA, Roberts BW, Richter DJ, Fairclough SR, King N. Origin of metazoan cadherin diversity and the antiquity of the classical cadherin/beta-catenin complex. *Proc. Natl. Acad. Sci. USA.* 2012; 109:13046–13051. [PubMed: 22837400]
31. Nakagawa T, Pellegrino M, Sato K, Vosshall LB, Touhara K. Amino acid residues contributing to function of the heteromeric insect olfactory receptor complex. *PLOS ONE.* 2012; 7:e32372. [PubMed: 22403649]
32. Darling JA, et al. Rising starlet: the starlet sea anemone, *Nematostella vectensis*. *BioEssays.* 2005; 27:211–221. [PubMed: 15666346]
33. Rentzsch F, Fritzenwanker JH, Scholz CB, Technau U. FGF signalling controls formation of the apical sensory organ in the cnidarian *Nematostella vectensis*. *Development.* 2008; 135:1761–1769. [PubMed: 18441276]
34. Magie CR, Daly M, Martindale MQ. Gastrulation in the cnidarian *Nematostella vectensis* occurs via invagination not ingression. *Dev. Biol.* 2007; 305:483–497. [PubMed: 17397821]
35. Kraus Y, Technau U. Gastrulation in the sea anemone *Nematostella vectensis* occurs by invagination and immigration: an ultrastructural study. *Dev. Genes Evol.* 2006; 216:119–132. [PubMed: 16416137]
36. Sinigaglia C, Busengdal H, Leclere L, Technau U, Rentzsch F. The bilaterian head patterning gene *six3/6* controls aboral domain development in a cnidarian. *PLOS Biol.* 2013; 11:e1001488. [PubMed: 23483856]
37. Nakanishi N, Renfer E, Technau U, Rentzsch F. Nervous systems of the sea anemone *Nematostella vectensis* are generated by ectoderm and endoderm and shaped by distinct mechanisms. *Development.* 2012; 139:347–357. [PubMed: 22159579]

38. Richards GS, Rentzsch F. Transgenic analysis of a *soxB* gene reveals neural progenitor cells in the cnidarian *Nematostella vectensis*. *Development*. 2014; 141:4681–4689. [PubMed: 25395455]
39. Kusserow A, et al. Unexpected complexity of the Wnt gene family in a sea anemone. *Nature*. 2005; 433:156–160. [PubMed: 15650739]
40. Tu Q, Cameron RA, Worley KC, Gibbs RA, Davidson EH. Gene structure in the sea urchin *Strongylocentrotus purpuratus* based on transcriptome analysis. *Genome Res*. 2012; 22:2079–2087. [PubMed: 22709795]
41. Burke RD, et al. A genomic view of the sea urchin nervous system. *Dev. Biol*. 2006; 300:434–460. [PubMed: 16965768]
42. Marlow H, et al. Larval body patterning and apical organs are conserved in animal evolution. *BMC Biol*. 2014; 12:7. [PubMed: 24476105]
43. Santagata S, Resh C, Hejnal A, Martindale MQ, Passamaneck YJ. Development of the larval anterior neurogenic domains of *Terebratalia transversa* (Brachiopoda) provides insights into the diversification of larval apical organs and the spiralian nervous system. *EvoDevo*. 2012; 3:3. [PubMed: 22273002]
44. Liu J, et al. *C. elegans* phototransduction requires a G protein-dependent cGMP pathway and a taste receptor homolog. *Nat. Neurosci*. 2010; 13:715–722. [PubMed: 20436480]
45. Edwards SL, et al. A novel molecular solution for ultraviolet light detection in *Caenorhabditis elegans*. *PLOS Biol*. 2008; 6:e198. [PubMed: 18687026]
46. Hedges SB, Dudley J, Kumar S. TimeTree: a public knowledge-base of divergence times among organisms. *Bioinformatics*. 2006; 22:2971–2972. [PubMed: 17021158]
47. Churcher AM, Taylor JS. The antiquity of chordate odorant receptors is revealed by the discovery of orthologs in the cnidarian *Nematostella vectensis*. *Genome Biol. Evol*. 2011; 3:36–43. [PubMed: 21123836]
48. Roy S, et al. Identification of functional elements and regulatory circuits by *Drosophila* modENCODE. *Science*. 2010; 330:1787–1797. [PubMed: 21177974]
49. Moresco JJ, Koelle MR. Activation of EGL-47, a Galphao-coupled receptor, inhibits function of hermaphrodite-specific motor neurons to regulate *Caenorhabditis elegans* egg-laying behavior. *J Neurosci*. 2004; 24:8522–8530. [PubMed: 15456826]
50. Waterhouse RM, Tegenfeldt F, Li J, Zdobnov EM, Kriventseva EV. OrthoDB: a hierarchical catalog of animal, fungal and bacterial orthologs. *Nucleic Acids Res*. 2013; 41:D358–365. [PubMed: 23180791]
51. Krogh A, Larsson B, von Heijne G, Sonnhammer EL. Predicting transmembrane protein topology with a hidden Markov model: application to complete genomes. *J. Mol. Biol*. 2001; 305:567–580. [PubMed: 11152613]
52. Sievers F, et al. Fast, scalable generation of high-quality protein multiple sequence alignments using Clustal Omega. *Mol. Syst. Biol*. 2011; 7:539. [PubMed: 21988835]
53. Waterhouse AM, Procter JB, Martin DM, Clamp M, Barton GJ. Jalview Version 2--a multiple sequence alignment editor and analysis workbench. *Bioinformatics*. 2009; 25:1189–1191. [PubMed: 19151095]
54. Guindon S, Dufayard JF, Lefort V, Anisimova M, Hordijk W, Gascuel O. New algorithms and methods to estimate maximum-likelihood phylogenies: assessing the performance of PhyML 3.0. *Syst. Biol*. 2010; 59:307–321. [PubMed: 20525638]
55. Le SQ, Gascuel O. An improved general amino acid replacement matrix. *Mol. Biol. Evol*. 2008; 25:1307–1320. [PubMed: 18367465]
56. Anisimova M, Gascuel O. Approximate likelihood-ratio test for branches: A fast, accurate, and powerful alternative. *Syst. Biol*. 2006; 55:539–552. [PubMed: 16785212]
57. Oliveri P, Carrick DM, Davidson EH. A regulatory gene network that directs micromere specification in the sea urchin embryo. *Dev. Biol*. 2002; 246:209–228. [PubMed: 12027443]
58. Rast JP, Amore G, Calestani C, Livi CB, Ransick A, Davidson EH. Recovery of developmentally defined gene sets from high-density cDNA macroarrays. *Dev. Biol*. 2000; 228:270–286. [PubMed: 11112329]
59. Fritzenwanker JH, Technau U. Induction of gametogenesis in the basal cnidarian *Nematostella vectensis* (Anthozoa). *Dev. Genes Evol*. 2002; 212:99–103. [PubMed: 11914942]

60. Saina M, Technau U. Characterization of myostatin/gdf8/11 in the starlet sea anemone *Nematostella vectensis*. *J. Exp. Zool. B Mol. Dev. Evol.* 2009; 312:780–788. [PubMed: 19533681]
61. Minokawa T, Rast JP, Arenas-Mena C, Franco CB, Davidson EH. Expression patterns of four different regulatory genes that function during sea urchin development. *Gene Expr. Patterns.* 2004; 4:449–456. [PubMed: 15183312]
62. Hejnol A, et al. Assessing the root of bilaterian animals with scalable phylogenomic methods. *Proc. R. Soc. Lond. B Biol. Sci.* 2009; 276:4261–4270. [PubMed: 19759036]

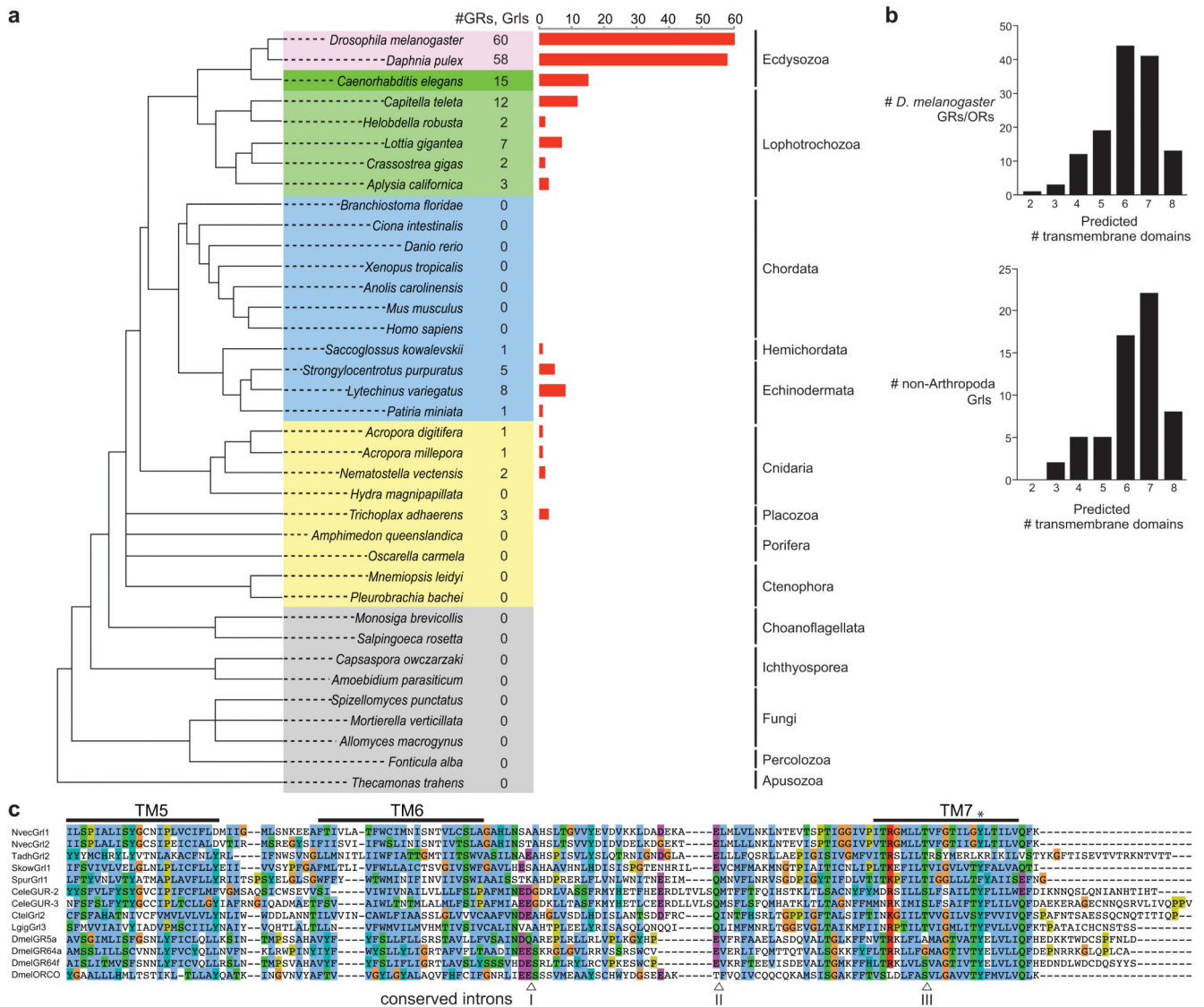


Figure 1. Identification of Gr-like (Grl) genes

(a) Summary of the *GR/Grl* repertoires identified in the genomes of selected arthropods (pink), non-arthropod Ecdysozoa (dark green), Lophotrochozoa (light green), Deuterostomia (blue) and non-Bilateria (yellow). An unscaled tree showing the phylogenetic relationships between these species is illustrated on the left; relationships among the different non-bilaterian phyla is unresolved, with the exception of the Cnidaria, which are the closest sister group to Bilateria⁶². Related genes were identified in multiple species of nematode worms but, for simplicity, only *C. elegans* is shown.

(b) Computational predictions of the number of transmembrane domains found in *D. melanogaster* GRs and ORs (top) and Grls (bottom). Grl sequence fragments (lacking start/stop codons) were excluded from this analysis.

(c) Alignment of the C-terminal regions of select insect GRs and ORs, *C. elegans* GURs and Grls. Predicted transmembrane (TM) domains are indicated with horizontal lines. The asterisk marks a conserved tyrosine residue important for ion conduction in insect ORs³¹.

The arrowheads below the alignment indicate the positions of three phase 0 ancestral GR introns (inferred from analysis of *D. melanogaster* GRs and ORs¹) that are conserved in *Grls*: intron I is conserved in phase and position in *NvecGrl1*, *NvecGrl2*, *TadhGrl2*, *SpurGrl1*, *CeleGUR2*, *CeleGUR3*, *CtelGrl2*, *LgigGrl3*; intron II is conserved in phase and position in *NvecGrl1*, *NvecGrl2*, *TadhGrl2*, *SpurGrl1*, *CtelGrl2*, and *LgigGrl3*. Intron III is conserved in all sequences.

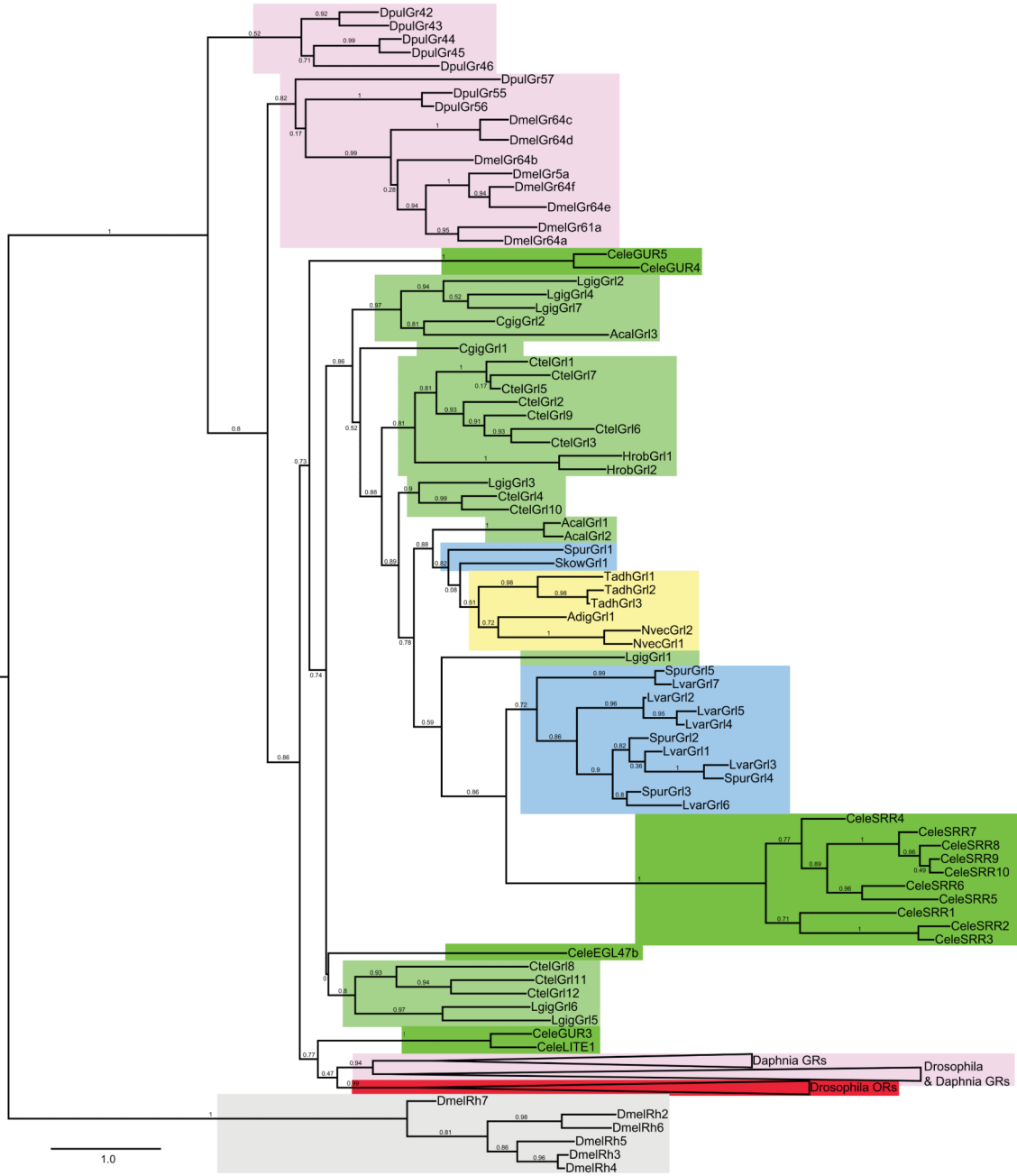


Figure 2. Phylogenetic analysis of Gr1, GR and OR genes
 Maximum likelihood tree showing the relationships between select arthropod GRs/ORs, *C. elegans* GURs and all Gr1s (except the short sequence fragments predicted in *P. miniata* and *A. millepora*), colour-coded as in Fig. 1a. *Drosophila* Rhodopsins are included as an outgroup; although it remains unclear whether these two different families of heptahelical membrane proteins share a common ancestor, they clearly belong to a separate clade. For clarity, branches for large clades of *D. melanogaster* GRs/ORs or *D. pulex* GRs have been collapsed. The scale bar represents the number of amino acid substitutions per site.

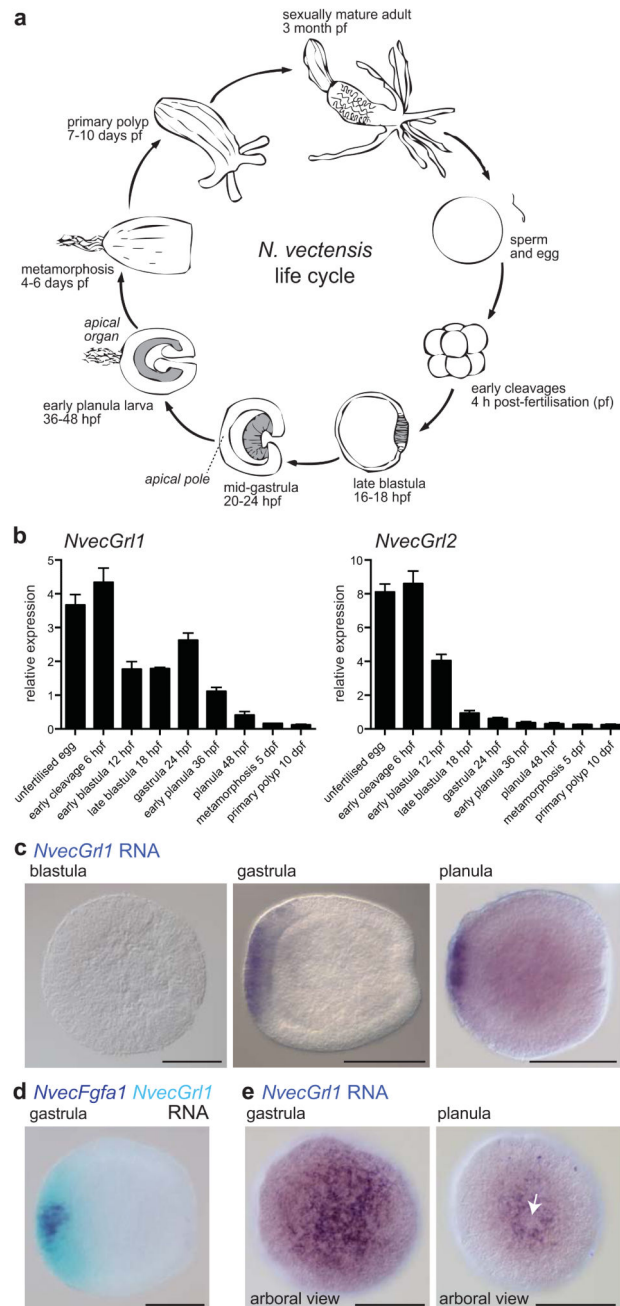


Figure 3. *N. vectensis* Gr1s are expressed during early development

(a) Schematic of the life cycle of the sea anemone *N. vectensis*. Dark grey shading in blastula, gastrula and early planula stages indicates the endoderm.

(b) Quantitative RT-PCR analysis of the temporal expression of *NvecGr1* and *NvecGr2* during nine developmental time-points. Data from three biological replicate samples (mean \pm s.e.m.) are shown.

- (c) RNA *in situ* hybridisation using a riboprobe against *NvecGrll* on whole mount *N. vectensis* at three developmental stages. Lateral views, with the arboral side on the left, are shown for all specimens in this and subsequent figures, unless otherwise noted.
- (d) Two-colour RNA *in situ* hybridisation using riboprobes against *NvecGrll* (light blue) and *NvecFgfa1* (dark blue) on whole mount *N. vectensis* embryos.
- (e) RNA *in situ* hybridisation using a riboprobe against *NvecGrll* on whole mount *N. vectensis* at two developmental stages showing an apical view, which reveal the formation of a ring-like distribution of transcripts at the planula stage. The apical organ forms from the unstained cells inside the ring (white arrow). Scale bars in (c-e) = 100 μ m.

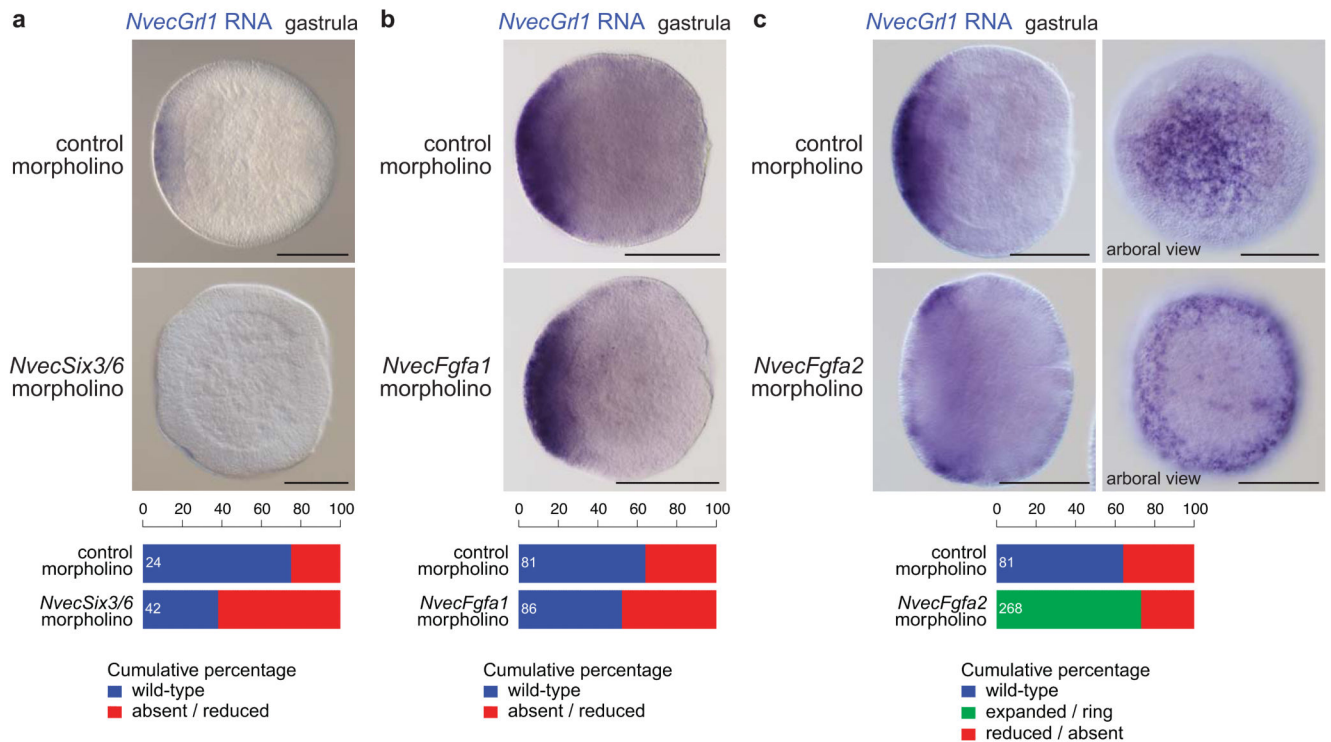


Figure 4. Regulation of *N. vectensis* Grl1 expression by the apical patterning network

(a) RNA *in situ* hybridisation using a riboprobe against *NvecGr1* on whole mount *N. vectensis* embryos injected with either control or *NvecSix3/6* morpholino oligonucleotides.

Quantification of the phenotypes is shown below. Note that *NvecGr1* transcripts are relatively weakly detected and a fraction of control morpholino injected animals did not exhibit staining. The n is shown in white within each bar in this and all equivalent graphs.

(b) RNA *in situ* hybridisation using a riboprobe against *NvecGr1* on whole mount *N. vectensis* embryos injected with either control or *NvecFgfa1* morpholino oligonucleotides. Quantification of the phenotypes is shown below.

(c) RNA *in situ* hybridisation using a riboprobe against *NvecGr1* on whole mount *N. vectensis* embryos injected with either control or *NvecFgfa2* morpholino oligonucleotides. In *NvecFgfa2* morphants, note the precocious formation and larger size of the ring of *NvecGr1* transcripts around the aboral pole (compare with Fig. 3e). Quantification of the phenotypes is shown below. Scale bars in (a c) = 100 μ m.

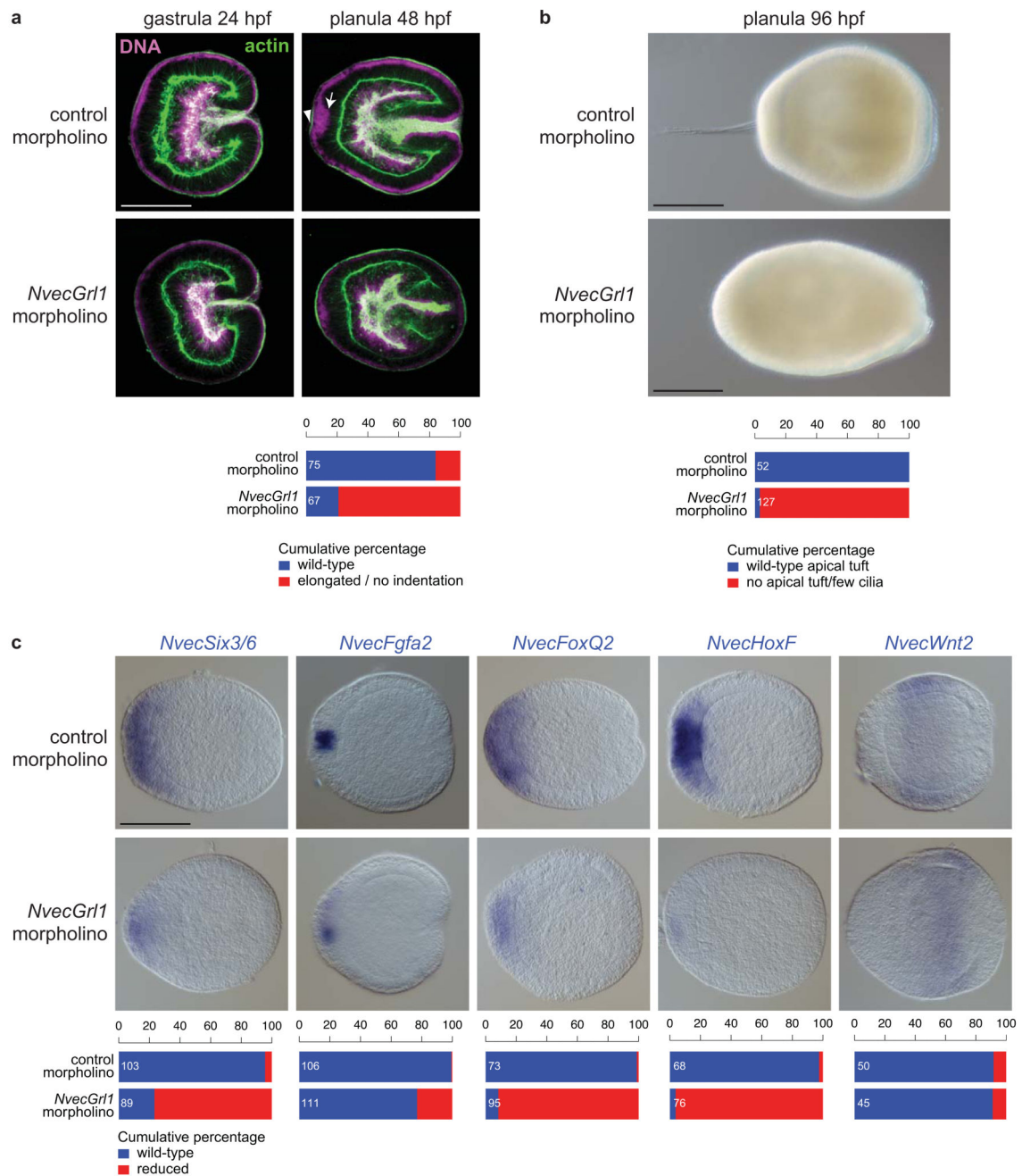


Figure 5. *N. vectensis* Gr1 is required for arboreal pole patterning

(a) Morphological phenotypes of *N. vectensis* embryos injected with either control (control#1) or *NvecGr1* (*NvecGr1*#1) morpholino oligonucleotides, in which DNA (magenta) and the actin cytoskeleton (green) are labelled with TO-PRO-3 and Alexa Fluor 488 Phalloidin, respectively. The arrow marks the group of nuclei at the aboral pole that have translocated to a more basal position (towards the right of the image) in control but not *NvecGr1* morphants; this results in these cells forming a small indentation of the apical

ectoderm (arrowhead). Scale bar = 100 μm (applies to all images). Quantification of the phenotypes is shown below.

(b) Bright-field images of living 4 day planulae derived from *N. vectensis* embryos injected with either control (control#1) or *NvecGr11* (*NvecGr11*#2) morpholino oligonucleotides revealing the failure in apical tuft develops in *NvecGr11* morphants. Quantification of the phenotypes is shown below. Scale bars = 100 μm .

(c) RNA *in situ* hybridisation using probes against marker genes in animals injected with either control (control#1) or *NvecGr11* (*NvecGr11*#1) morpholino oligonucleotides. Scale bar = 100 μm (applies to all images). Quantification of the phenotypes is shown below.

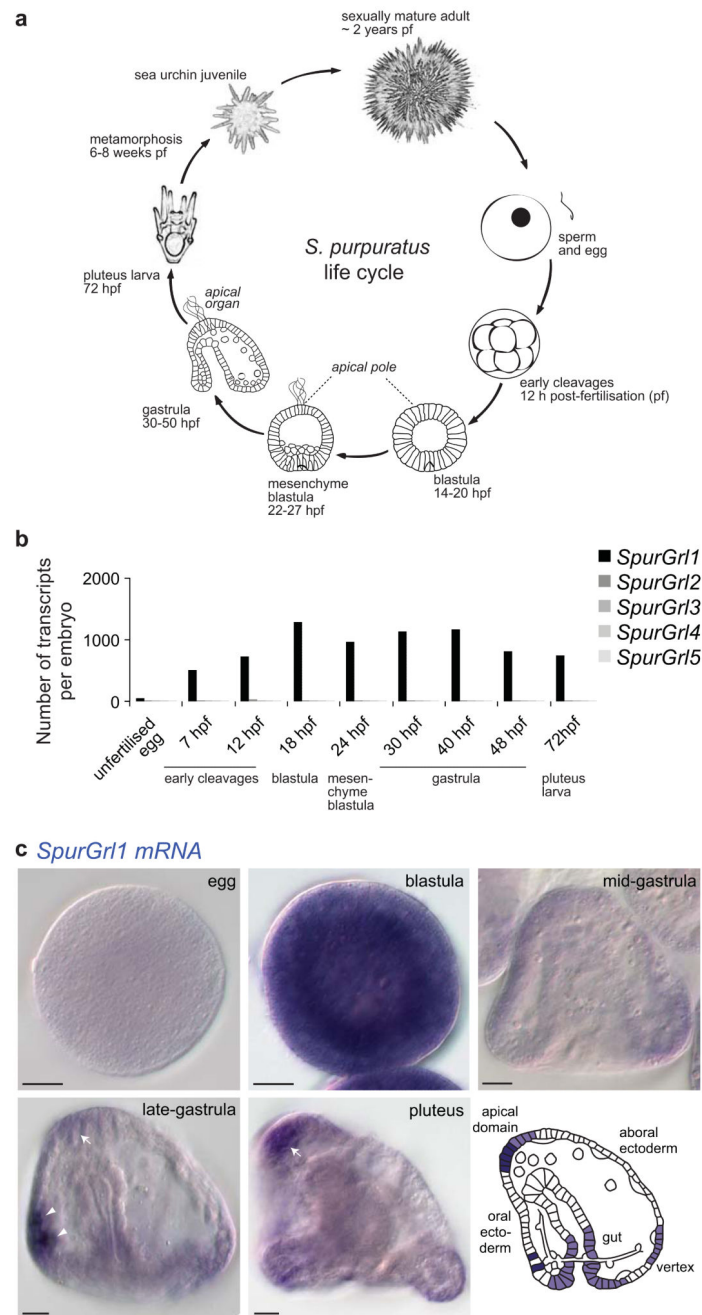


Figure 6. Early developmental expression of an *S. purpuratus* Grl

(a) Schematic of the life cycle of the sea urchin *S. purpuratus*.

(b) Quantitative RT-PCR analysis of the temporal expression of the five *SpurGrl* genes during nine developmental time points. Data are represented as number of transcripts per embryo and represent the average of four technical replicates in each of two independent biological replicate samples (see Supplementary Table 3).

(c) RNA *in situ* hybridisation using a riboprobe against *SpurGrl1* on whole mount *S. purpuratus* of five developmental stages. All the embryos represent lateral views: as

indicated in the schematic, the oral ectoderm is on the left and the apical domain on the top in gastrula and pluteus specimens. The arrows mark the expression of *SpurGr11* in the apical domain (where the apical organ will form), while the arrowheads mark a pair of presumptive neurosecretory cells in the oral ectoderm. Scale bars = 20 μm .